



VIBRATIONAL PROCESSES IN THE BALLAST LAYER UNDER NON-STATIONARY LOAD CONDITIONS

Krasnov, Oleg G., JSC Rolling Stock Research, Design and Technology Institute (AO VNIKTI), Moscow, Russia.

Bogdanov, Oleg K., JSC Rolling Stock Research, Design and Technology Institute (AO VNIKTI), Moscow, Russia.

ABSTRACT

This article presents the results of experimental research of vibrational processes in the ballast layer at the depths of 100 mm and 200 mm below the sleeper sole under non-stationary loads caused by

percussive interaction between the wheels with faults in the form of flat spots on the tread, and the rails. Dependencies are established of vibrational accelerations on the values of vertical percussive loads on the rail caused by faulty wheels.

Keywords: railway track, vibrational processes, non-stationary loading, percussive forces, accelerations, crushed stone fragments, ballast layer, wheel faults.

Background. Non-stationary modes of loading emerging in the interaction between the rail and wheels that have faults on their treads are a factor that causes intensive deterioration of a track under train load. Experimental and theoretical studies are known that look into the processes of vibrational impact on granular media, including crushed stone ballast of a railway [1–4].

with six measurement modules that performed continuous measurement of vertical forces. On the neutral axis of either rail, 48 resistive strain sensors spaced at 130 mm were glued on the inner and outer sides.

This article discusses the results of our studies of dynamic and vibrational processes induced in the contact area of the wheel and the rail, and in the ballast layer, under the impact of percussive forces created by wheels with faults.

Installation diagrams for the vertical force measurement resistive strain modules, and a general view of the experimental segment are shown in Figures 1 and 2.

As such percussive forces impact the rails, vibrational dynamic processes are induced in the elements of the track's upper structure, including the ballast layer. These processes reduce the internal friction between ballast particles, cause «vibrational fluidity» in granular media, and intensify setting of the ballast layer.

To obtain quantitative values of the vibrational fields induced in the ballast layer depending on the magnitudes of percussive forces, acceleration levels in the ballast layer were measured. To this end, simulated ballast particles were made of an epoxy resin as irregularly shaped particles 50–70 mm in size inside which KD-35 vibration sensors were installed in mutually perpendicular positions. The sensors were connected to vibration amplifiers and then to with the MIC-026 measurement system (manufactured by NPP MERA Research and Production Association).

Objective. The objective of the authors is to consider vibrational processes in the ballast layer under non-stationary load conditions.

The simulated crushed stone particles with embedded vibration sensors were installed in the ballast at the level of 100 mm ± 10 mm below the sleeper sole, and at the depth of 200 mm ± 10 mm, and were oriented in relation to the vertical and longitudinal horizontal axes of the track. Three measurement modules were used in order to determine the positioning of the percussive force zones.

Methods. The authors use general scientific and engineering methods, experimental methods, graph construction, evaluation method.

A diagram showing the positioning of the simulated crushed stone particles is presented in Figure 3.

Results.

Research setup

To study vibrational processes in the ballast layer with due account of vertical forces, an experimental segment was selected on the Golutvin-Ozyory run of the Moscow Railway.

For the period of the research, an experimental train was formed consisting of two 2TE116 locomotive units, an experimental car, and a laboratory car (Figure 4).

The characteristics of the segment are presented in Table 1.

To evaluate the forces involved in the interaction between the wheels and the rails, both rails were fitted

Vibration measurements were performed as the loaded tank car with wheels having faults in the form of a wheel flat was passing. The faults on the treads

Table 1

Characteristics of the segment

Characteristic	Value of the characteristic
Track	straight, continuous welded rail
Rails	P65
Sleepers	reinforced concrete
Fasteners	KB-65, standard tensioning
Sleeper density	at least 1,840 pieces per 1 km
Ballast	crushed hard stone, fractions 25 to 60 mm
Rail canting	from 1/20 to 1/22
Speed range, km/h	up to 90

Table 2

Geometric parameters of flat spots

Fault	Geometric parameters of the spot, mm	
	Depth	Length*
Flat spot	1	64
	2	87
	3	101
	4	129

*Chord length of the flat spot

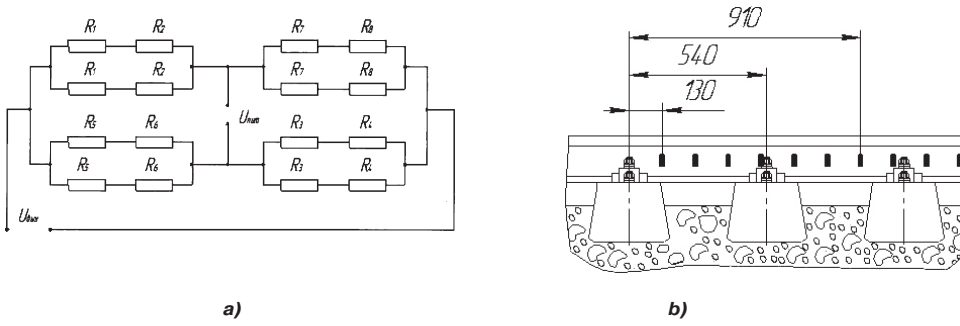


Figure 1. Diagram of a vertical force continuous measurement module: a) wiring diagram; b) installation of strain sensors on the rail.



Figure 2. General view of the track equipped with vertical force measurement instruments.

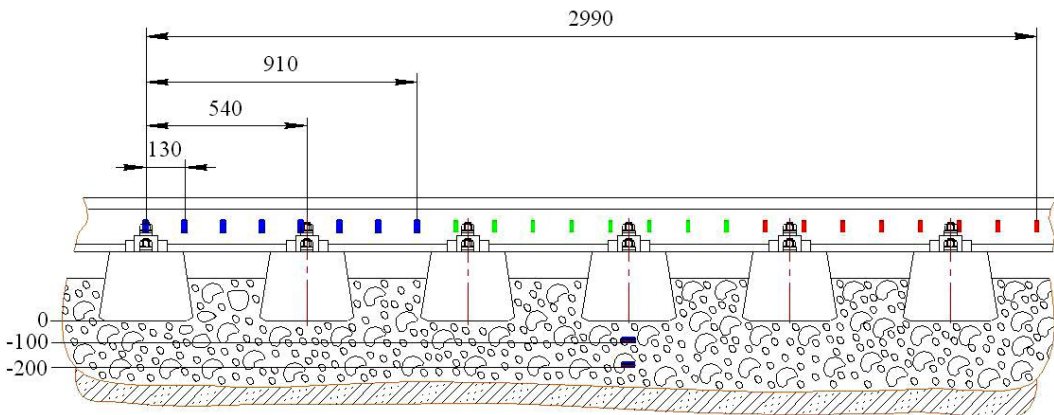


Figure 3. Positioning diagram of simulated crushed stone particles with embedded vibration sensors.

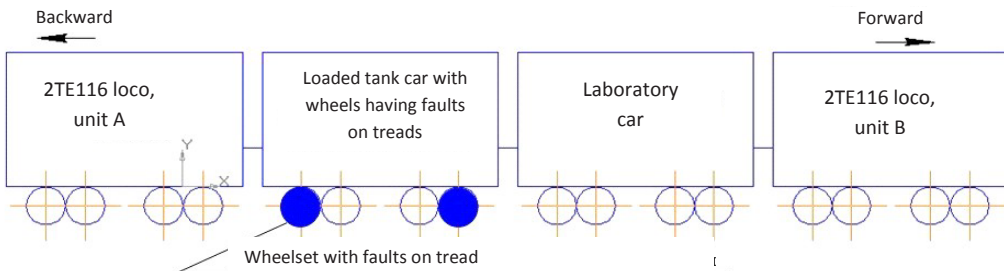


Figure 4. Experimental train composition.



Average and maximal values of forces of interaction between wheels with flat spots and the railway track for summer conditions of operation

Speed of railway vehicle movement V , km/h	Geometric dimensions of flat spot, mm		Maximal value of vertical force, kN	Minimal value of vertical force, kN	Mathematical expectation of force of interaction between the wheel and the rail m_p , kN	Standard deviation of vertical percussive forces σ , kN	Value of maximal percussive force, $P_{prob}^{max} = m_p + 3\sigma$, kN
	depth h	length l					
1.1*	1	64			108		
	2	87			112		
	3	101			127		
	4	129			147		
32	1	64	284	145	210	43	338
	2	87	290	194	242	35	347
	3	101	386	290	330	32	426
	4	129	567	346	465	65	659
42	1	64	265	153	188	39	306
	2	87	300	210	261	31	355
	3	101	415	307	374	34	476
	4	129	550	392	463	52	620
49	1	64	271	191	237	35	343
	2	87	307	225	262	37	373
	3	101	440	320	366	52	522
	4	129	547	373	455	85	710
60	1	64	296	183	261	43	391
	2	87	320	220	272	38	387
	3	101	440	300	361	53	520
	4	129	622	563	602	23	672
70	1	64	271	193	241	32	336
	2	87	289	239	262	20	323
	3	101	431	292	373	58	548
	4	129	641	447	551	67	752
79	1	64	269	180	197	31	289
	2	87	280	220	252	30	342
	3	101	400	300	336	46	474
	4	129	550	400	484	51	638

* A single passage at the speed of 1.1 km/h was made for the purpose of calibrating the sensors.

of the wheelset were artificially made at the AO VNIKTI industrial facility.

The geometric parameters of the flat spots are specified in Table 2.

For the experiments, two flat spots with the depths of 4 mm and 1 mm positioned at 180° relative to each other were formed on the left wheel of the first wheelset. On the left wheel of the fourth wheelset of the other bogie, 3 and 2-mm deep flat spots positioned diametrically opposite each other were similarly formed. Such a positioning of the wheelsets in the front and rear bogies of the tank car made it possible to view them as the leading wheelsets whether the car moved forward or backward (cf. Figure 4).

Measurements were performed as the loaded car (the tank car) was passing the measurement segment forward and backward at speeds of 30–80 km/h, at the speed increment of 10 km/h. For each speed, at least five iterations of the measurements in either direction were made. Prior to the experiments, the measurement channels were calibrated by the vertical forces by means of rolling the experimental train at a speed of 1–1.5 km/h, with known wheel load values.

Outcomes of the experiment

Levels of vertical forces applied to the rails. In the course of the research, the forces of interaction between the wheels with faults and the railway track in the summer conditions of operation were determined by experiment.

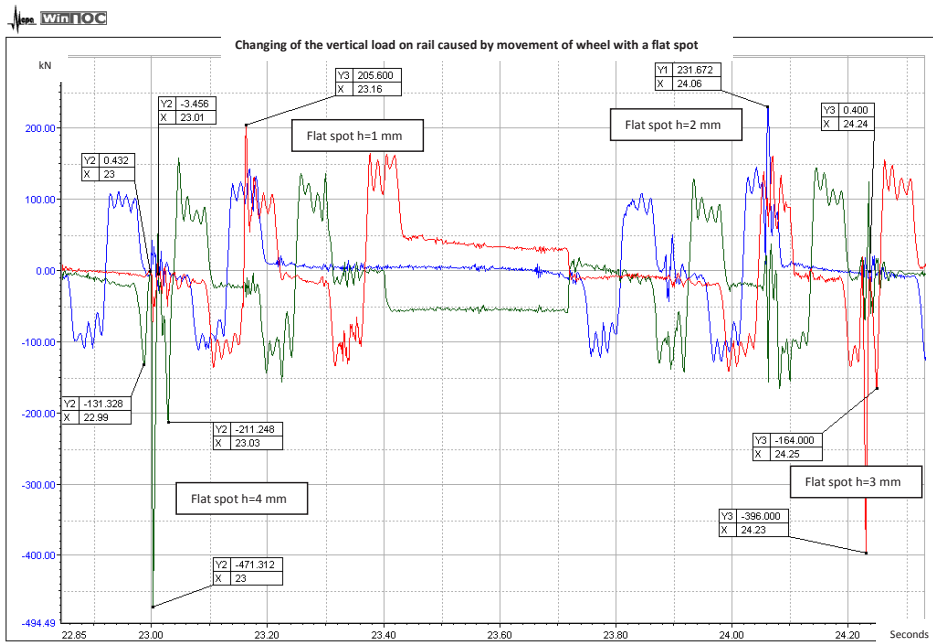


Figure 5. Impact of wheels with faults in the form of flat spots on the rail at the experimental train speed of 32 km/h.

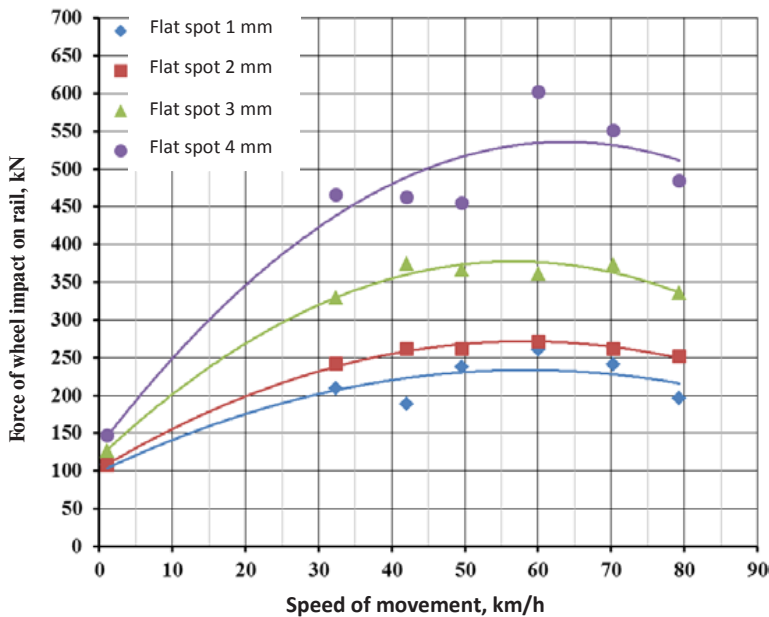


Figure 6. Graphs of variance of the vertical load (average) on the rail from a faulty wheel depending on the size of the flat spot and the speed of movement.

Figure 5 shows a typical curve reflecting the process of impact to the rail caused by the wheels with faults in the form of flat spots at the speed of 32 km/h.

As the wheels with 1, 2, 3, and 4 mm-deep flat spots interact with the rail, percussive pulses are generated whose magnitudes during the passages of the experimental car were 206, 232, 396, and 471 kN, respectively.

The process of a wheel with a flat spot moving on the rail was characterized with a period of wheel unloading from the beginning of its turn relative to the end of a flat spot to the moment of its contact with the rail when a percussive pulse was initiated. For the 4 mm deep flat spot, the duration of the unloading

period was 0.0156 seconds, with the magnitude of the percussive pulse reaching 471 kN. The actual time intervals and the amplitudes of the vertical forces are determined by the sizes and shapes of flat spots, the speed of movement, the stiffness of the permanent way, and the static load on the wheel with a flat spot.

The distribution of the vertical forces was mapped according to their statistical characteristics such as their maximal, minimal, and average values as well as their standard deviations. The values of the vertical forces and their statistical parameters for various flat spots depths and various speeds of movement are presented in Table 3.

Figure 6 shows the curves of change in the average value of the vertical percussive load on the



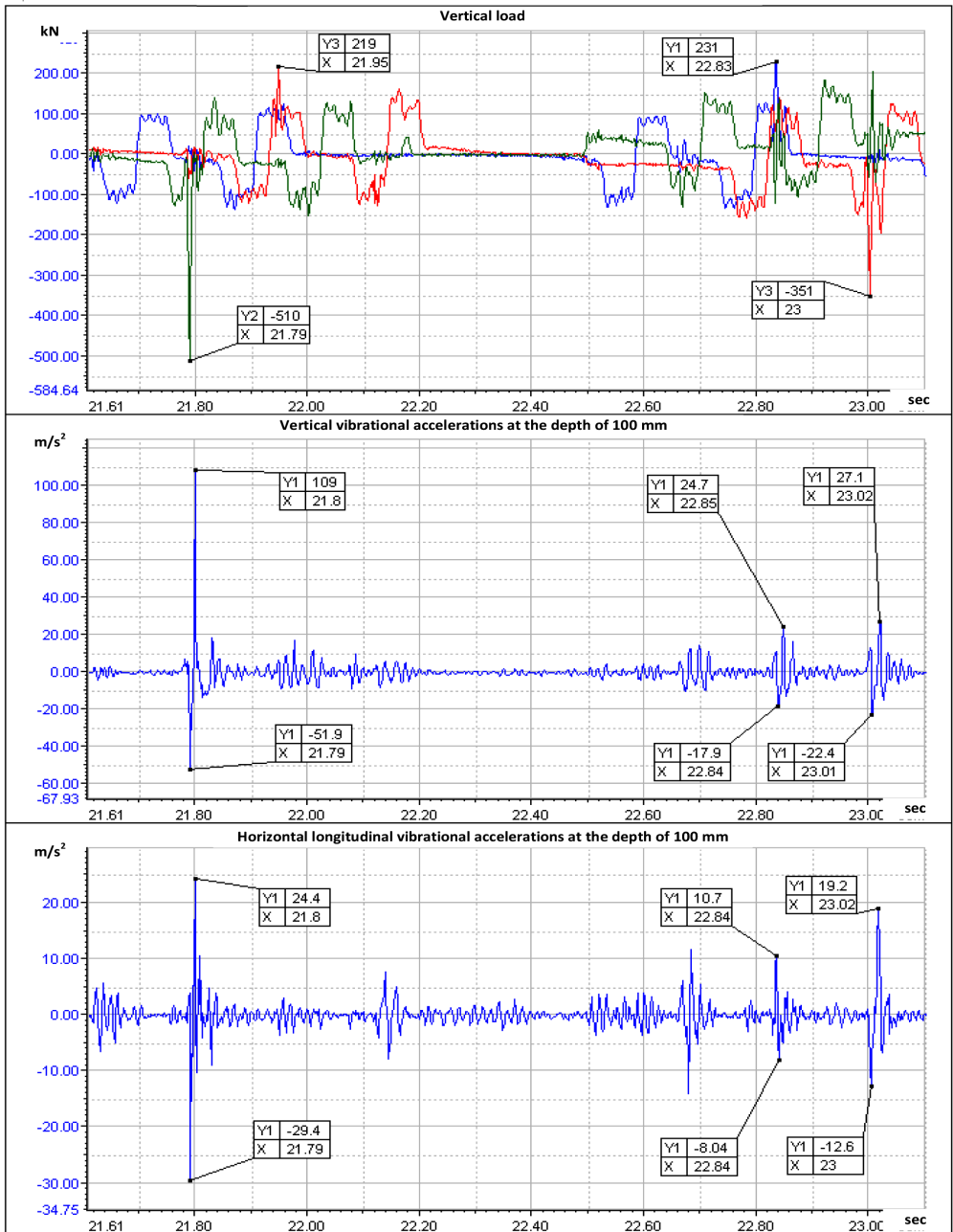


Figure 7. Vertical vibrational accelerations of crushed stone particles in the ballast layer at the depth of 100 mm from sleeper soles caused by wheels with flat spots.

rail caused by a faulty wheel depending on the size of the flat spot and the speed of movement. The curves demonstrate that the vertical load on the rail grows as the speed increases, reaching the maximal value at speeds of 55–65 km/h. With further growth of the speed of movement, the vertical force on the rail caused by a wheel with a flat spot decreases.

Levels of vibrational accelerations in the ballast layer. The behavior of the dynamic processes emerging in the ballast layer under the percussive interaction between wheels with flat spots and the rails is illustrated in Figure 7.

The process of change in the vertical and longitudinal vibrational accelerations of ballast particles is similar to and concurrent with the process of vertical force impact on the rail.

Reviewed below are the most representative measured parameters of vibrations in the ballast layer caused by the impact of the wheels with flat spots.

When the experimental car was moving at a speed of 32 km/h, the percussive pulse of 510 kN was measured by the nearest sensor located at a distance of 0.3 m.

The pulse was transmitted to the elements of the permanent way, with an increase in both vertical and longitudinal accelerations. By their nature, the dynamic processes of vertical accelerations were identical to those that would be caused by an impact of a force.

At the moment of wheel unloading, the acceleration is directed opposite to the direction of elastic rebound of the rail-and-sleeper assembly, i.e. downward. At this point, the acceleration reached $W_{vert.1}^n = -51.9 \text{ m/s}^2$. As the wheel reestablishes its interaction with the rail, the percussive pulse is directed downward. At this moment, the accelerations change their directions to the opposite, with their values reaching $W_{vert.2}^n = 109 \text{ m/s}^2$ and their range $W_{vert.}^{ange} = 160 \text{ m/s}^2$ (16-g).

Longitudinal accelerations increased synchronously but their levels were weaker, from 1/4 to 1/2 of the vertical accelerations, which is due to the direction of the impact. The pattern of longitudinal acceleration was closer to a symmetric cycle as compared with the asymmetric vertical acceleration.

The oscillatory process had an evanescent nature on both the vertical and longitudinal axes (fading out in 0.02–0.03 s) because of the significant damping in the granular medium of the crushed stone ballast.

The next spike in the oscillation was of a significantly lower level than the first one, and was observed after a half-turn of the wheel at $t = 0.17 \text{ s}$. At the speed of the experimental train of 31.8 km/h, this corresponded to a travel of approximately 1.5 m and the interaction of the flat spot of $h = 1 \text{ mm}$ with the rail. The oscillatory process consisted of a set of 5–6 oscillations with vibration levels of $W_{vert.2} = 12\text{--}18 \text{ m/s}^2$ and $W_{long.2} = 3\text{--}4 \text{ m/s}^2$. Another half-turn later ($\sim 3 \text{ m}$), the next interaction of the flat spot of $h = 4 \text{ mm}$ with the rail was observed as it increased the accelerations of ballast particles. However, the accelerations did not exceed $W_{vert.3} = W_{long.3} < 5\text{--}6 \text{ m/s}^2$. As the train moved on, the oscillatory process in the crushed stone particles associated with the percussive impact was discontinued. Thus, in a powerful percussive interaction (in our case, involving a flat spot of $h = 4 \text{ mm}$), waves of vibration were spreading to a distance of up to 3 m, engaging particles of the ballast layer in an oscillatory process.

The vibration graphs show periodic areas of increased vertical and longitudinal accelerations defined by the regular periodic impacts of the wheel with flat spots.

With tread faults in the form of a flat spot of $h = 1 \text{ mm}$, the vertical vibration levels were recorded as $W_{vert.1} = 22.4\text{--}27.1 \text{ m/s}^2$, longitudinal as $W_{long.1} = 12.8\text{--}19.2 \text{ m/s}^2$, which is 1/4 to 1/2 of the levels caused by a flat spot of $h = 4 \text{ mm}$. The lower vibration levels are explained with weaker percussive forces generated by a flat spot of $h = 1 \text{ mm}$ that were recorded as $P_{perc} = 180\text{--}220 \text{ kN}$.

With flat spots of $h = 2$ and 3 mm , the oscillatory process retained its pattern while the accelerations had intermediate values to those measured with flat spots of $h = 4$ and 1 mm .

Figure 8 presents dot charts of vertical accelerations of crushed stone particles at the depths of 100 mm and 200 mm below the sleeper sole, directed down (a) and up (b), with the acceleration range shown in chart (c), relative to the vertical percussive force caused by the interaction of the wheels with flat spots with the rail. Only those acceleration values were adopted that were caused by percussive pulses recorded immediately above, or in a very close vicinity of, the vibration sensors.

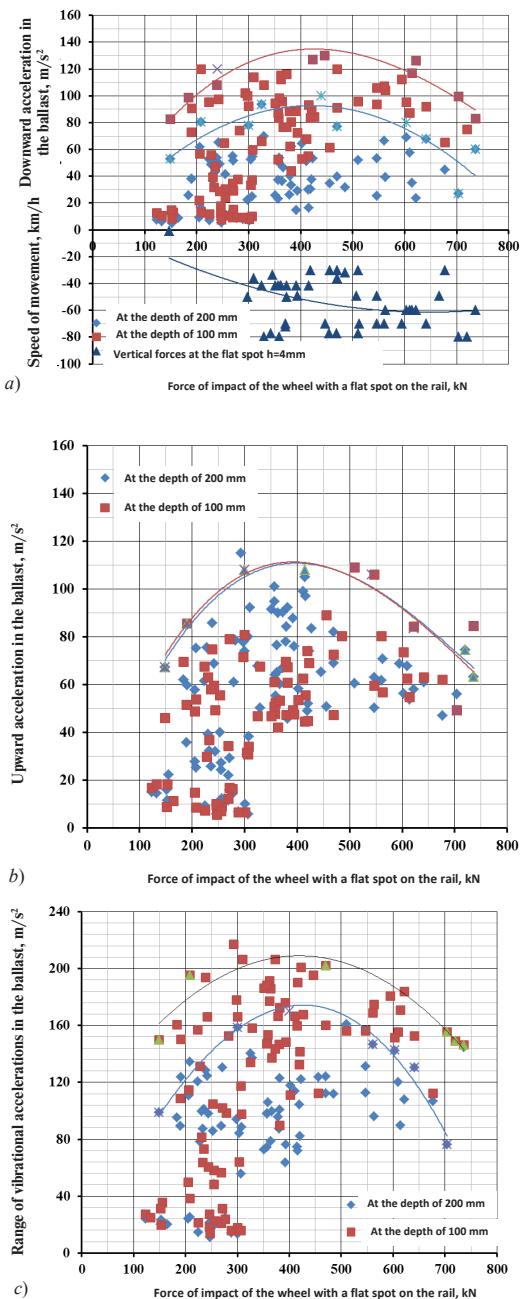


Figure 8. Dot charts of vertical accelerations of crushed stone particles at the depths of 100 mm and 200 mm below the sleeper sole directed downward (a) and upward (b) relative to the vertical percussive impact, and the range of acceleration values.

All the diagrams contain envelope curves drawn by the maximal values of vibrational accelerations since such maximal accelerations have the greatest effect on the stability of the ballast.

Our analysis of the experimental data indicates the following:

- vertical accelerations are proportional to the magnitude of the percussive force impact of the faulty wheel on the rail;
- in line with the existing tendency toward the maximal increase of the force impact of flat spots in



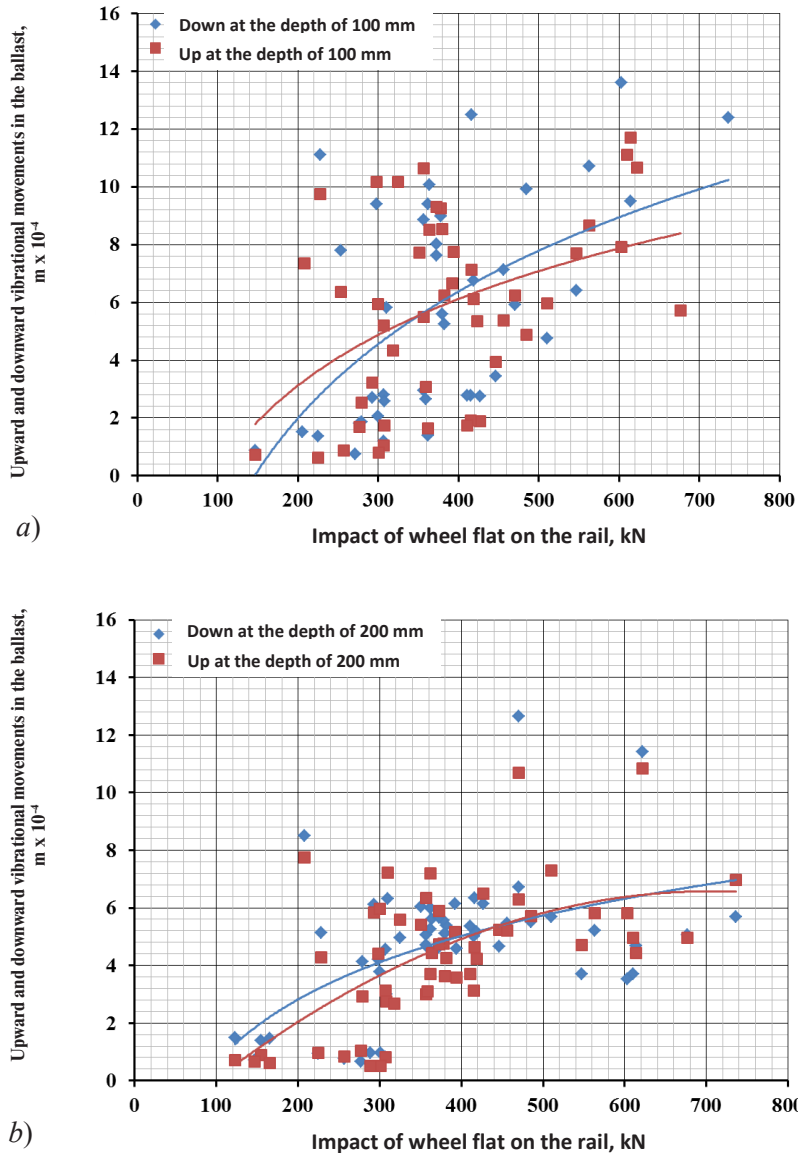


Figure 9. Dot charts of vertical vibrational movements of crushed stone particles at the depths of 100 mm (a) and 200 mm (b) below the sleeper sole, directed downward and upward relative to the vertical percussive load.

the speed range from 40 to 50 km/h, a particular consistent pattern existed in the range of accelerations of crushed stone particles;

- the dot charts show a considerable scatter in the accelerations of crushed stone particles, which is explained by the scatter of the force impacts caused by the faulty wheels to the rail during repeat passages, the random distribution of distances between the point of impact of the wheel fault on the rail and the cross section in which the acceleration sensors are installed;

- as the depth at which the crushed stone particles were located was increased from 100 mm to 200 mm, the observed levels of vibration tended to be reduced by 15–30 %. However, because of the scatter in the acceleration values, there were cases when such values exceeded the accelerations of crushed stone particles located at the depth of 100 mm in the same conditions of testing. On the

whole, observed in a greater sample was a tendency toward lower acceleration levels as the depth of particles' location increased, which is due to the attenuation of the percussive waves as they propagated in a granular medium;

- a comparative analysis of downward accelerations induced by the interaction of flat spots with the rail revealed a significant difference in the values of such accelerations at different depths, which reconfirms the probabilistic nature of the process;

- on the vertical axis, the oscillatory process is asymmetric, with upward accelerations having greater values. On the longitudinal axis, acceleration values are on average 1,5–2,5 of the vertical ones, with the process being closer to a symmetric cycle.

Together with the accelerations of crushed stone particles, their vibrational movements were determined.

Presented in Figure 9 are dot charts of vertical vibrational movements of crushed stone particles at the depths of 100 mm and 200 mm below the sleeper soles, which movements were directed downward (Figure 10a) and upward (Figure 10b) relative to the percussive vertical load created by the interaction of wheel flats with the rail.

Our analysis of the experimental data indicates the following:

- vibrational movements of crushed stone particles have a steady tendency to increase as the vertical percussive forces grow;
- at equal levels of percussive forces, vibrational movements of crushed stone particles vary widely. Thus, at $P_{vert}^{perc} = 300$ kN, vertical movements of crushed stone particles varied within the range of 0.1–1.1 mm for downward movements, and 0.05–0.72 mm for upward movements. This phenomenon can be explained with the non-linearity of granular media characteristics;
- there are differences between the levels of downward vibrational movements (in the same direction as the direction of the percussive force) and the upward movements (the direction of elastic rebound). The differences between upward and downward vibrational movements provide evidence that, apart from the elastic deformation under percussive impacts, there exists residual deformation of the ballast layer. The greater the percussive force, the greater are the differences between upward and downward movements, and the greater the residual deformation.

Conclusion

As a result of the research, the values of forces of interaction between wheel flats and the rail under summer conditions of operation were obtained in experiments. Our analysis indicates that:

- percussive interactions between wheel flats and the rails are a powerful factor inducing vibrations in the ballast layer, which reduces the coefficient of effective friction in the ballast layer and leads to intense residual setting and deterioration of the track;
- under percussive impact of wheels on the rail, crushed stone particles engage in three-dimensional oscillations; on the vertical axis, the oscillatory process is asymmetric, with greater intensity in the downward direction, and smaller intensity in the upward direction; longitudinal oscillations are harmonic, with an insignificant asymmetry coefficient;
- the levels of vibrations are determined by the force of the percussive interaction that depends on the type of the fault, its geometric dimensions, the speed of movement, and on the distance from the source of the percussive impact. As the distance grows, the levels of vibration diminish. Under a powerful percussive impact (e.g. from a wheel flat of $h = 4$ mm), the waves of vibration propagate to distances of over 3 m;
- the oscillatory process in the ballast has the form of a rapidly evanescent process due to the high damping coefficient of the granular medium; an

acceleration pulse caused by a percussive force fades out practically after the first oscillation.

REFERENCES

1. Popov, S. N. On Allowable Stresses on Ballast [*O dopuskaemykh napryazheniyah na ballast*]. *Interaction of Track and Rolling Stock and Questions of Track Calculation. Collection of scientific works*, Iss. 97. Moscow, Transzheldorizdat publ., 1955, pp. 353–384.
2. Prokudin, I. V., Kolos, A. F., Kozlov, I. S., Nikolaistist, D. S. Sensitivity of crushed stone ballast to vibrodynamic effects [*Chuvstvitel'nost' shhebjonochno ballasta k vibrodinamicheskomu vozdejstviyu*]. *Railway track design and maintenance issues of high-speed main lines. Proceedings of international scientific-practical seminar* / ed. by L. S. Blazhko. St. Petersburg, PSTU publ., 2010, pp. 71–72.
3. Kolos, A. F., Nikolaistist, D. S., Morozova, A. A. Assessment of sensitivity of track rubble to the action of vibrodynamic load [*Ocenka chuvstvitel'nosti putevogo shhebnya k dejstviyu vibrodinamicheskoy nagruzki*]. *Modern problems of design, construction and operation of a railway track: Proceedings of the 10th scientific-technical conference*. Moscow, MIIT publ., 2013, pp. 164–166.
4. Krasnov, O. G., Akashev, M. G., Efimenko, A. V., et al. Influence of shock forces on vibration in the ballast layer [*Vlijanie udarnykh sil na vibracii v ballastnom sloe*]. *Put' i putevoe hozjajstvo*, 2013, Iss. 3, pp. 5–10.
5. Morozova, A. A. The bearing capacity of the railroad track padded base on the areas of train turnover with axial loads up to 300 kN. Ph.D. (Eng.) thesis [*Nesushhaja sposobnost' podshpal'nogo osnovanija zheleznodorozhnogo puti na uchastkah obrashhenija poezdov s osevyimi nagruzkami do 300 kN / Dis... kand. tehn. nauk*]. St. Petersburg, PSTU publ., 2014, 184 p.
6. Tretyakov, V. V. Influence of characteristics of the subballast base on the intensity of accumulation of track disorders in the vertical plane. Ph.D. (Eng.) thesis [*Vlijanie harakteristik podballastnogo osnovanija na intensivnost' nakoplenija rasstrojstv puti v vertikal'noj ploskosti / Dis... kand. tehn. nauk*]. Moscow, JSC VNIIZhT, 2008, 150 p.
7. Tursunov, Kh. I. Study of oscillatory process in the ballast prism, clogged with barkhan sands [*Issledovanie kolebatel'nogo processa v ballastnoj prizme, zasorenoy barhannymi peskami*]. *Inzhenernyj vestnik Dona*, 2012, Iss. 3, pp. 358–389.
8. Baraboshin, V. F., Lysyuk, V. S. Improvement of vibroprotective properties of the track with reinforced concrete sleepers [*Uluchshenie vibrozashhitnykh svoystv puti s zhelezobetonnymi shpalami*]. *Vestnik VNIIZhT*, 1980, Iss. 1, pp. 48–51.
9. Baraboshin, V. F., Ananiev, N. I. Increase of stability of a track in a zone of a rail joint [*Povyshenie stabil'nosti puti v zone rel'sovogo styka*]. Moscow, Transport publ., 1978, 45 p.
10. Pevzner, V. O., Zheleznov, M. M., Kaplin, V. N., et al. Increase of stability of track in the joint zone due to the use of elastic padded gaskets [*Povyshenie stabil'nosti puti v zone stykov za schet primeneniya uprugih podshpal'nykh prokladok*]. *Vestnik VNIIZhT*, 2016, Iss. 3, pp. 140–146.

Information about the authors:

Krasnov, Oleg G. – Ph.D. (Eng.), Head of Track and Special Railway Vehicles Department of JSC Rolling Stock Research, Design and Technology Institute (AO VNIKT), Moscow, Russia, krasnovog@mail.ru.

Bogdanov, Oleg K. – Ph.D. (Eng.), Leading Engineer of Operational Testing Laboratory, Track and Special Railway Vehicles Department of JSC Rolling Stock Research, Design and Technology Institute (AO VNIKT), Moscow, Russia, bogdanov_ok@mail.ru.

Article received 24.10.2016, accepted 28.12.2016.

